Contents lists available at ScienceDirect

Journal of Environmental Management

journal homepage: www.elsevier.com

Research article

Impact of secondary inorganic aerosol and road traffic at a suburban air quality monitoring station

L. Megido [a], L. Negral [b, *], L. Castrillón [a], Y. Fernández-Nava [a], B. Suárez-Peña [c], E. Marañón [a]

[a] Department of Chemical and Environmental Engineering, Polytechnic School of Engineering, Gijón Campus, University of Oviedo, 33203 Gijón, Spain
[b] Department of Chemical and Environmental Engineering, Technical University of Cartagena, 30202 Cartagena, Spain
[c] Department of Materials Science and Metallurgical Engineering, Polytechnic School of Engineering, Gijón Campus, University of Oviedo, 33203 Gijón, Spain

ARTICLE INFO

Article history:
Received 29 September 2016
Received in revised form 3 December 2016
Accepted 12 December 2016
Available online xxx

Keywords:
African dust outbreak
Combustion
Natural apportionment
Particulate matter
SIA
Suburban air pollution

ABSTRACT

PM10 from a suburban site in the northwest of Spain was assessed using data from chemical determinations, meteorological parameters, aerosol maps and five-day back trajectories of air masses. Temporal variations in the chemical composition of PM10 were subsequently related to stationary/mobile local sources and long-range transport stemming from Europe and North Africa.

The presence of secondary inorganic species (sulphates, nitrates and ammonium) in airborne particulate matter constituted one of the main focuses of this study. These chemical species formed 16.5% of PM10 on average, in line with other suburban background sites in Europe. However, a maximum of 47.8% of PM10 were recorded after several days under the influence of European air masses. Furthermore, the highest values of these three chemical species coincided with episodes of poor air circulation and influxes of air masses from Europe. The relationship between SO_4^{2-} and NH_4^+ ($R^2 = 0.57$, p-value<0.01) was found to improve considerably in summer and spring ($R^2 = 0.88$ and $R^2 = 0.87$, respectively, p-value<0.01), whereas NO_3^- and NH_4^+ ($R^2 = 0.55$, p-value<0.01) reproduced this pattern in winter ($R^2 = 0.91$, p-value<0.01). The application of a receptor model to the dataset led to the identification of notable apportionments due to road traffic and other types of combustion processes. In fact, large amounts of particulate matter were released to the atmosphere during episodes of biomass burning in forest fires. On isolated days, combustion was estimated to contribute up to 21.0 μg PM/m^3 (50.8% of PM10). The contribution from industrial processes to this source is also worth highlighting given the presence of Ni and Co in its profile. Furthermore, African dust outbreaks at the sampling site, characterised by an arc through the Atlantic Ocean, were usually associated with a higher concentration of Al_2O_3 in PM10.

Results evidenced the relevance of stationary (i.e., steelworks and thermal power station) and mobile sources in the air quality at the suburban site under study, with important apportionments of particulate matter coming from road traffic and as consequence of releasing precursor gases of secondary particles to the atmosphere.

1. Introduction

Human activities influence environmental sustainability. The release of pollutants to the environment must be managed in a way that reduces their impact on ecosystems (Schaubroeck et al., 2016). In particular, air quality plans have to be designed to abate gaseous precursors of secondary aerosol (inorganic and organic), which represents between 40 and 71% of PM10 in Europe depending on the location (Amato et al., 2016).

In the case of secondary inorganic aerosol (SIA), which includes sulphates, ammonium and nitrates, the gas-to-particle transformation is the most important contributor (Sun et al., 2015). The origin of its precursor gases (NO_X, SO_X and NH_3) may be either natural or anthropogenic. These gases may be released by local sources or originate from distant locations as a result of long-range transport, the latter being highly dependent on weather conditions (Di Gilio et al., 2015). Moreover, secondary inorganic compounds could be more concentrated during African dust outbreaks, together with mineral dust and other trace elements (Fernández-Camacho et al., 2016). The contribution of different sources to airborne particulate matter (PM) has been widely estimated in air quality studies via the application of what are known as receptor models (Jorquera and Barraza, 2013; Taiwo et al., 2014). These statistical approaches are based on pollutant concentrations determined at a sampling location (receptor site) and do not require direct measurements or emission inventories as in other types of source apportionment methodologies (Alleman et al., 2010). Examples of broadly implemented receptor models are Principal Component Analysis (PCA) and Positive Matrix Factorization (PMF) (Fernández-Olmo et al., 2016).

Although it is not necessary to characterise each possible source of PM to apply a receptor model (Padoan et al., 2016), it is essential to infer the emission sources correctly from the principal components provided by the models. The commonly named marker elements or tracers provide clues regarding the sources that may be associated with each factor given by the model. The perfect tracer would be unique to one source, constant (regardless of operational and environmental conditions), inert and very precisely measured (Khalil and

* Corresponding author.
Email address: luis.negral@upct.es (L. Negral)

http://dx.doi.org/10.1016/j.jenvman.2016.12.032
0301-4797/

Rasmussen, 2003). Nevertheless, it is not unusual to find the same element reported in the literature as a tracer of several sources, thus giving rise to dissimilar conclusions (Taiwo et al., 2014). Given PM is highly influenced by meteorology (Li et al., 2016), the aforementioned difficulty can be overcome via the study of meteorological factors that affect air quality. Dispersion of pollutants in the atmosphere, wind, solar radiation and topography are amongst the most important (Di Gilio et al., 2015). Some of these factors are essential to assess the seasonal behaviour of secondary species.

The aim of this study was to identify relevant sources of PM10 at a suburban location where road traffic and nearby industrial activities were thought to influence air quality. Special attention was paid to secondary inorganic species and days with higher levels of pollution, when these species represented the largest fraction of PM10. To this end, results from a receptor multivariate model, several meteorological parameters, five-day back trajectories of air masses and aerosol maps were simultaneously analysed. Variations in the chemical composition of PM10 were subsequently related to stationary/mobile local sources and long-range transport stemming from Europe and North Africa. Results were compared with other studies carried out in the area that used a different approach and with other European suburban background sites in order to provide useful information for managing air quality.

2. Materials and methods

2.1. Receptor site

The sampling area was situated at a suburban site (43º31′23.1″N 5º37′16.2″W) in the east of Gijón, a city in north-western Spain. Fig. 1 shows the location of the sampling station, as well as the main industrial activities in the area: port facilities, a cement plant, coalfield, coal-fired power plant, steelworks and industrial complexes. Activities at the complexes encompass aluminium production, galvanizing, the manufacture of refractory products, iron casting, the melting of aluminium scrap and the production of metallic structures and wires (Gobierno del Principado de Asturias, 2014).

2.2. Gravimetrical and chemical determinations

Three hundred and seventy-five daily samples of PM10 were collected over microfibre filters during the period July 2013–July 2014, using a high-volume sampler MCV CAV-A/MSb (30 m^3/h). The filter material was composed of either glass or quartz microfibres. PM10 levels were gravimetrically determined from all the samples. Fifty-two PM10 samples were collected over quartz matrixes once a week and, subsequently, chemically processed to analyse their composition. The sampling day was alternated to obtain samples of all days of the week, thirteen samples being collected at weekends and twenty-three during raining days (above 1.0 mm).

2.2.1. Analytical and indirect determinations

The PM10 samples were acid digested; Al, As, Ba, Be, Bi, Ca, Cd, Ce, Co, Cr, Cu, Fe, K, La, Li, Mg, Mn, Mo, Na, Ni, Pb, Rb, Sb, Se, Sn, Sr, Ta, Ti, Tl, V, Zn and Zr in PM10 were determined by inductively coupled plasma mass spectrometry. Organic and elemental carbon (OC and EC) were quantified by means of a thermo-optical method. Ion chromatography was used to analyse four soluble chemical species (Cl^-, NH_4^+, NO_3^- and SO_4^{2-}). Al_2O_3 was stoichiometrically calculated from Al. Organic matter (OM) was estimated from organic carbon (OC), applying a factor of 1.2, which has been used in sampling locations close to traffic (Amato et al., 2016). Further details about the equipment and the methodology are provided in the supplementary material.

2.3. Receptor model: PCA-MLRA

The receptor model used to study source apportionment was PCA, applying Statistica software. The chemical compositions of the fifty-two samples were used in the PCA, twenty-eight chemical species being introduced in the analysis as variables (see supplementary material). Varimax rotation, a procedure to maximise the explained variance, was used to explore the relationship between variables. Principal components with eigenvalues higher than 1 were retained, as in Negral et al. (2008). Multi-Linear Regression Analysis (MLRA) was used to model PM10 as the dependent variable, as well as the concentration of the chemical species used in the PCA. The percent

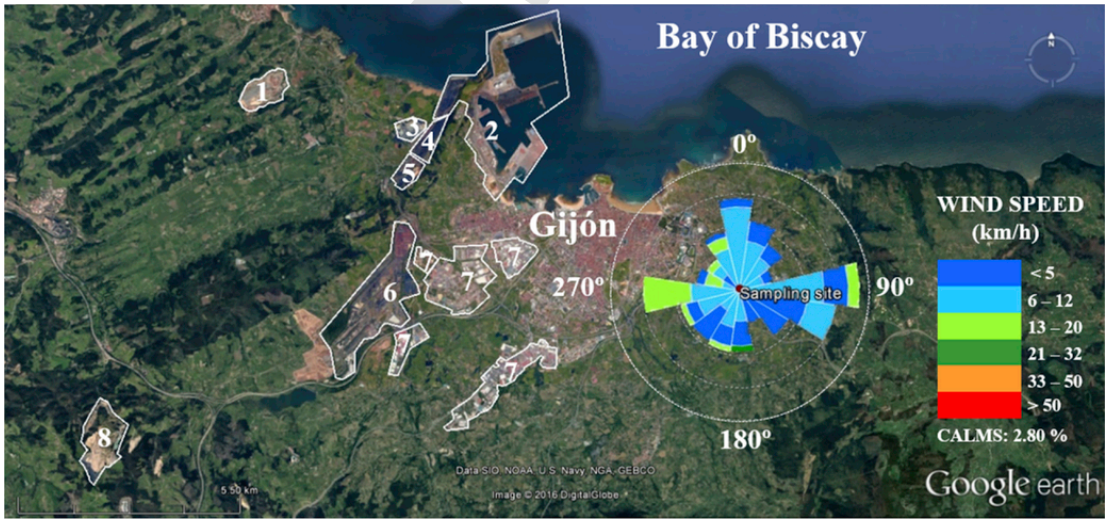

Fig. 1. Wind rose and location of the sampling site and nearby industrial activities: 1) limestone quarry; 2) port facilities; 3) cement plant; 4) coalfield; 5) coal-fired power plant; 6) steelworks; 7) industrial complexes; and 8) landfill.

age contribution of a specific factor to the predicted PM10 was calculated as the sum of the predicted PM10 for the fifty-two samples for this factor divided by the total concentration of predicted PM10 considering all factors.

2.4. Meteorological parameters

Fig. 1 shows the wind rose obtained from data recorded at the sampling location by the Spanish Meteorology Agency (AEMET) since October 2013. The predominant wind directions between October 2013 and July 2014 were East, Southeast and West. Information from AEMET on maximum wind speed and wind direction for each sampling day was used to build polar plots of the concentration of the analysed chemical species in PM10. These graphs were useful in identifying their most likely sources, given that they would be situated in the wind directions that have higher values (Yi and Hwang, 2014). Other tools used to support data interpretation were: dust concentrations predicted by the SKIRON forecasting model, images from the BSC-DREAMS8b model, the NAAPS Global Aerosol Model and the analysis of five-day isentropic back trajectories (ending at 12:00 UTC) calculated at three heights (750, 1500, 2500 m above sea level) with HYSPLIT model from NOAA (Stein et al., 2015). The study of five-day back trajectories led to classifying the air mass origin as Northern Atlantic (AN), North-western Atlantic (ANW), Western Atlantic (AW), South-western Atlantic (ASW), Northern African (NAF), Mediterranean (ME), European (EU), and Regional (RE).

3. Results and discussion

Sulphates, nitrates and ammonium, together with the carbonaceous fraction, were the major components of PM10 in the east of Gijón. In a previous study (Megido et al., 2016c), carbonaceous particles were found predominant in the coarse fraction of PM, being mainly deposited in the extrathoracic region of the human respiratory tract. In the case of sulphates and nitrates, Li et al. (2016) found that were mainly in the fine size fraction of PM (i.e., PM1), which implies that they would reach deeper regions of the respiratory system, thereby posing a health risk.

Sulphates, nitrates and ammonium represented more than 4% on average of the overall PM10 mass (SO_4^{2-}: 6.5%; NO_3^-: 4.4%; NH_4^+: 5.6%), the contribution from SO_4^{2-} being the most notable, up to 22.1% of PM10 (Figs. S1 and S2). Fig. 2 presents a line chart of the PM10 levels determined in the fifty-two collected samples. Additionally, the stacked area chart indicates the total contribution of SIA to PM10, calculated as the sum of the individual apportionments of SO_4^{2-}, NO_3^- and NH_4^+ to PM10 in each sample. The contribution of each chemical species is differentiated inside the stacked area by means of a different pattern. These concentrations represented 16.5% of PM10 on average. The maximum (47.8% of PM10) was recorded on 16 March 2014 after several days (12–16 March 2014) with negligible precipitation rate (<1.0 mm) and influxes of air masses from Europe (EU), according to the HYSPLIT five-day back trajectories (Fig. 3). The NAAPS maps (Fig. 3) also shows the arrival of sulphates from the European continent.

Pey et al. (2009) found levels of SIA of 7.8 μg SIA/m^3 (27% of PM10) at a suburban site in Mallorca (Spain). These levels were high in comparison with those of other urban and industrial locations in northern Spain, but similar to those from regional and urban sites on the Spanish Mediterranean coast. Qadir et al. (2014) found that PMF factors of secondary sulphate and secondary nitrate presented similar contributions to PM10 (approximately 6.2 μg PM/m^3 and 4.3 μg PM/m^3, respectively) in eight urban/suburban/residential background sites studied during winter in Augsburg (Germany). Amato et al. (2016) highlighted the importance of secondary aerosol at an urban background site in Barcelona (Spain), where they found mean levels of 1.99 μg SO_4^{2-}/m^3, 1.99 μg NO_3^-/m^3 and 0.60 μg NH_4^+/m^3, the sum of these three accounting for 20.3% of PM10. Higher values were found at a suburban location in Athens (Greece), with 29.7% of PM10 on average. These authors pointed out the importance of reducing their gaseous precursors. In the surroundings of the sampling area, the main emitters of gaseous precursors of secondary particles were road traffic, steelworks, coal-fired power station and cement plant (Fig. 1). The three industries exceeded the notification threshold of NO_X in 2013 and 2014. The coal-fired power station and the steelworks also reported data on SO_X emissions, and the cement plant on NH_3 (PRTR-Spain[1]).

3.1. Seasonal pattern of secondary chemical species

The contribution of secondary inorganic species to PM10 was found to vary depending on the season (Table S3). SO_4^{2-}, NO_3^- and NH_4^+ showed greater variability in winter, when the mean daily temperatures fell within the 6.3–15.1 °C range (10.3 °C on average, n = 87 days). The minimum temperatures were as low as 0.4 °C, while the maximum temperatures reached up to 23.8 °C.

Sulphates presented the greatest mean concentration in summer (2.50 μg SO_4^{2-}/m^3) and the lowest in winter (1.06 μg SO_4^{2-}/m^3), reaching their limit values during these seasons (maximum: 7.10 μg SO_4^{2-}/m^3 on 1 August 2013 (<1 mm of precipitation); minimum: 0.14 μg SO_4^{2-}/m^3 on 4 February 2014 (4.0 mm of precipitation)). The maximum was recorded after two days (from 31 July 2013 to 1 August 2013) characterised by low air mass circulation, i.e., under RE. This situation combined with the fact that sulphates and nitrates remain in the atmosphere for 3–9 days (Belis et al., 2013), may explain the high levels registered. According to these authors, SO_4^{2-}, NO_3^- or NH_4^+ are usually associated with dust minerals or metals when applying PMF or PCA due to their similar residence time in the atmosphere.

The polar plot of sulphate concentrations as a function of the direction of maximum wind speed (Fig. 4) shows the highest levels originating from the sea, in the 330–45° sector (Fig. 1). These levels were recorded on days under EU, RE or AN. In general, the aforementioned air mass origins coincided with the highest levels of sulphates determined in PM10, with mean levels of 2.62 μg SO_4^{2-}/m^3, 2.25 μg SO_4^{2-}/m^3 and 1.83 μg SO_4^{2-}/m^3, respectively. The maximum levels reached under these conditions were 7.10 μg SO_4^{2-}/m^3 (1 August 2013), 4.61 μg SO_4^{2-}/m^3 (25 July 2014) and 3.70 μg SO_4^{2-}/m^3 (14 June 2014), respectively. Given the values recorded under EU, not only local emissions seemed to be relevant sources; long-range transport could also explain this pattern.

The seasonal trend observed in sulphate levels may be due to higher solar intensity during the warmest months of the year, favouring photochemical reactions that give rise to secondary sulphate (Sun et al., 2015). These authors found a strong relationship ($R^2 > 0.7$) between SO_4^{2-}–NH_4^+ and NO_3^-–NH_4^+ in a commercial and residential area of Seoul (Korea). In the present study, SO_4^{2-} and NH_4^+ presented a correlation with $R^2 = 0.57$ (p-value<0.01), which greatly improved in summer and spring (summer: $R^2 = 0.88$, spring: $R^2 = 0.87$, winter: $R^2 = 0.68$, autumn: $R^2 = 0.67$, p-values<0.01) (supplementary material).

[1] http://www.en.prtr-es.es/Informes/InventarioInstalacionesIPPC.aspx (Accessed 5 June 2016).

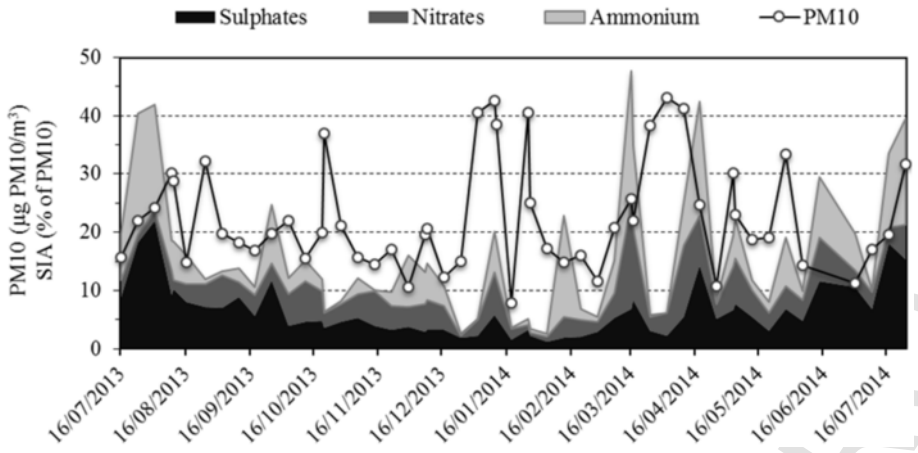

Fig. 2. PM10 (line chart) and SIA (stacked area chart displaying in different colours the percentage in which SO_4^{2-}, NO_3^- and NH_4^+ contributed to the overall SIA).

Nitrates also showed seasonality (Table S3), with greater concentrations during winter days (mean: 1.55 µg NO_3^-/m^3). The maximum value (7.87 µg NO_3^-/m^3) was determined on 16 March 2014, <1.0 mm of precipitation being recorded during this day and the previous twelve days. Due to the higher temperatures, NH_4NO_3 breaks down in summer to form HNO_3. In fact, the formation of secondary particles of this type is favoured by low temperatures and high humidity (Sun et al., 2015). These authors also reported a maximum (8.9 µg NO_3^-/m^3) in winter. As previously stated, sulphates presented low values on winter days in our study. Thus, the mass ratio of NO_3^-/SO_4^{2-} reached higher values during the coldest months of the year (up to 2.69 on 16 March 2014); the lowest values of the ratio being found in summer (summer: 0.36; autumn: 1.11; winter: 1.09; spring: 0.96). Li et al. (2016) reported high values of the NO_3^-/SO_4^{2-} ratio with pollution events and vehicle emissions in Beijing (China). In Seville (Spain), Fernández-Camacho et al. (2016) found variations in NO_2, a precursor of NO_3^- particles, which they related to road traffic emissions and atmospheric dynamics.

As for ammonium, its maximum during the sampling period was determined the same day as in the case of nitrates (9.80 µg NH_4^+/m^3 on 16 March 2014) and its minimum, in spring (0.01 µg NH_4^+/m^3 on 2 April 2014, 7.4 mm of precipitation being recorded this day and <1.0 mm in the previous six days) (Table S3). Furthermore, the highest levels of NH_4^+ and NO_3^- were found along the same directions of maximum wind speeds (0–45°) (Fig. 4) of air masses entering from the coast. As with sulphates, the highest values of nitrates and ammonium were recorded under EU (3.72 µg NO_3^-/m^3 on 10 April 2014 and 5.86 µg NH_4^+/m^3 on 1 August 2013), RE (7.87 µg NO_3^-/m^3 and 9.80 µg NH_4^+/m^3 on 16 March 2014) and AN (5.13 µg NO_3^-/m^3 and 5.8 µg NH_4^+/m^3 on 17 March 2014). The relationship between NO_3^- and NH_4^+ had a $R^2 = 0.55$ (p-value<0.01), being very strong in winter and weaker in summer (winter: $R^2 = 0.91$, p-value<0.01; spring: $R^2 = 0.52$, p-value<0.01; autumn: $R^2 = 0.34$, p-value<0.05; summer: $R^2 = 0.08$, p-value>0.05).

3.2. Sources of PM10 obtained by PCA-MLRA

Six factors were extracted using PCA which described 82% of the data variance. The factorial loading matrix is shown in Table 1; the main chemical species that supported the obtained factors have been highlighted in bold; i.e., loadings above 0.4, as in Godoy et al. (2005). Each factor was characterised by few of these chemical species, which are generally considered tracers of different sources as previously mentioned in the introduction section. On this basis, each factor was named in accordance with the associated source: 1) road traffic; 2) mineral dust and sulphates; 3) marine aerosol; 4) steelworks; 5) combustion; and 6) secondary aerosol. Table 1 also shows the contribution of each source to the total PM10 mass predicted by MLRA throughout the sampling period. The lineal correlation between the empirical data and the predicted PM10 presented a $R^2 = 0.92$ (p-value<0.01).

3.2.1. Factor 1: road traffic

The first factor explained 23.9% of the variance and was heavily loaded with Ba, Bi, Cu, EC, OM, Sn and Sb. EC and OC are commonly related to exhaust fumes from road traffic (Taiwo et al., 2014). Furthermore, this factor was consistent with the results obtained at the same location in a previous study aimed at identifying traffic tracers by means of elemental ratios and linear correlations (Megido et al., 2016a). All the aforementioned species were then associated with traffic, non-exhaust emissions (e.g., brake wear) being the most likely origin for Cu, Sb, and Sn. This showed that unsophisticated techniques based on simple mathematical calculations can be useful in source apportionment studies. The maximum levels of Factor 1 were predicted for working days, up to 20.15 µg PM10/m^3 on 17 December 2013. Yi and Hwang (2014) reported the highest values (10.35 µg PM10/m^3) of a factor characterised by OC, EC, Ca, Fe, K, Zn and Pb during weekdays, relating it to motor vehicles. Based on the above, Factor 1 was linked to road traffic.

Road dust re-suspension may explain the contribution of mineral elements such as Ca, Fe, K, Mn and Sr to this source (Jorquera and Barraza, 2013; Lin et al., 2016), although other possible origins cannot be ruled out. Srimuruganandam and Nagendra (2012) pointed to ash fractions of diesel exhausts to explain Ba, Zn, Fe, Al, K, Ca and Na^+ in PM10. Moreover, these researchers linked Zn and Ca to an oil component and Fe to several traffic-related sources: the doping of diesel with ferrocene, metal wear in the exhaust system, and road dust.

3.2.2. Factor 2: mineral dust and sulphates

Factor 2 represented 12.8% of the predicted PM10, with Al and Ti being major contributors. The origin of mineral dust could be local resuspension, African dust transport, fugitive emissions from quarries and/or road dust resuspension. This source may be characterised by several elements, such as Al, K, Ca, Fe, Mg, Li, Ti, Rb, Sr and Mn (Negral et al., 2008; Pandolfi et al., 2011; Yubero et al., 2011). In the present study, apart from Al and Ti, the rest of the aforementioned elements had low loadings in Factor 2, highlighting La and Ce instead.

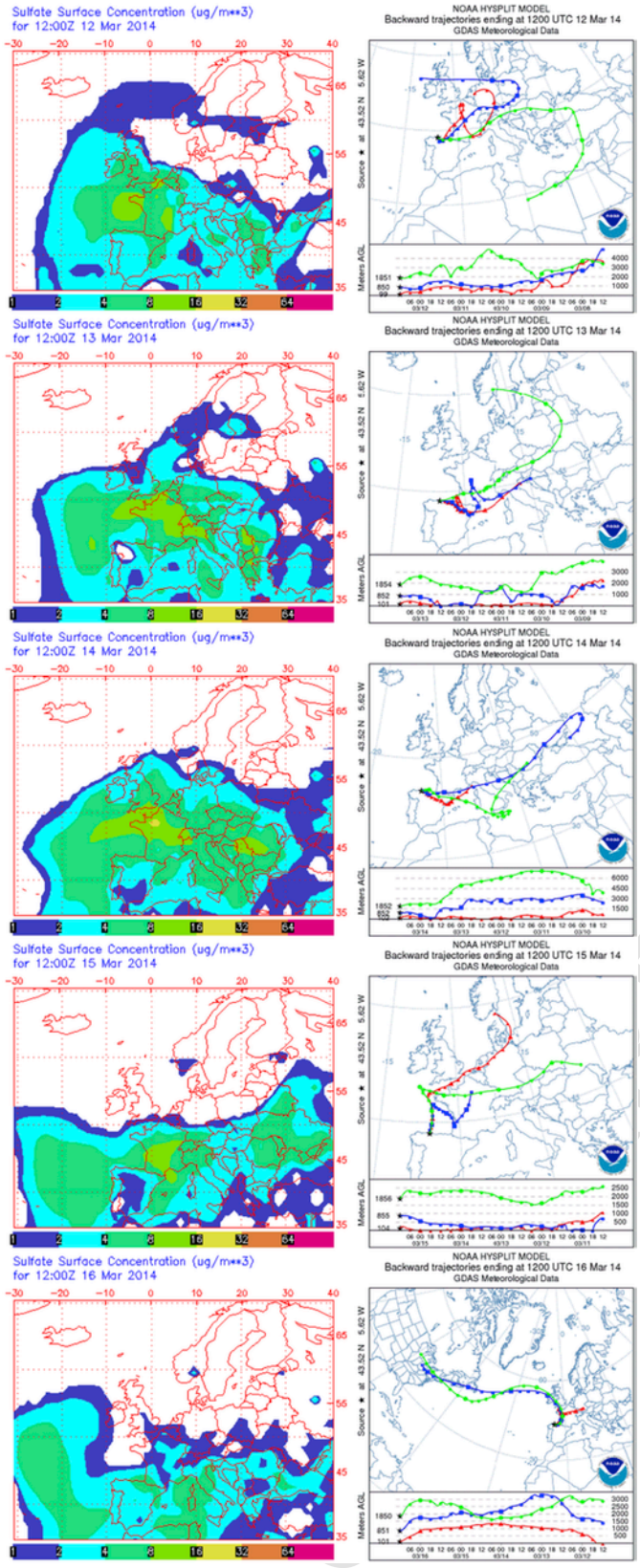

Fig. 3. Observation of sulphate-enriched European air masses reaching Gijón: NAAPS maps and HYSPLIT five-day back trajectories from 12 to 16 March 2014.

Padoan et al. (2016) applied different source apportionment techniques to infer the sources of PM10 in the Piedmont Region (Italy), explaining a factor mainly loaded by Ce and La as some kind of mineralogy association. Godoy et al. (2005) linked a factor, in which La and Ce had loadings of 0.9, with soil resuspension as a source of coarse particles. Lin et al. (2016) also reported that La is mainly linked to geological sources and petroleum refining. The latter source is ruled out in the present study, as no facilities of this type were located in the surroundings of the sampling area.

African dust outbreaks may be one of the possible sources of mineral PM in the study area in the northwest of Spain. Air masses from the African continent describe an arc through the Atlantic Ocean, crossing the Iberian Peninsula from northwest to southeast (Negral et al., 2012). Fig. 5 presents five-day back trajectories for the period 9–12 January 2014 when there was an African dust outbreak (MAGRAMA, 2015) describing the aforementioned scenario. The chemical composition of PM10 was analysed on 10 January 2014, 80%, 63%, 71% and 62% of the predicted Al_2O_3, Ti, La and Ce being respectively associated with Factor 2. Assuming their primarily soil origin of Al, Ti, La and Ce, Megido et al. (2016b) calculated enrichment factors using Al, Ti, La and Ce as reference elements to assess the anthropogenic influence on PM10 at this location, no major differences being found. It is worth mentioning that mineral dust is expected to have a lower contribution in finer fractions of PM, given that this component is predominant in the coarse fraction (Pérez et al., 2016).

Another African dust outbreak occurred on 12 and 13 December 2013 (MAGRAMA, 2014). No rainfall was registered during those days, nor on the following days. As the aforementioned days were under RE (i.e., poor air circulation), pollutant accumulation was favoured. SKIRON maps predicted a total dust load of 10–500 mg/m^2 and 1–10 μg/m^3 of dust concentration near the ground in the sampling area on 17 December 2013. That day, the PCA-MLRA model predicted that 4.6 μg PM10/m^3 was due to Factor 2, which represented 12.5% of the 37.0 μg predicted PM10/m^3, with a major contribution of Al_2O_3 (84% of total predicted Al_2O_3 for that day).

In general, Factor 2 reached maximum levels on days preceded by periods with a low precipitation rate, under EU or RE. The apportionment of this second factor to the overall predicted PM10 was relatively high (Table 1). This resulted from the contribution of sulphates to Factor 2. As previously stated, SO_4^{2-} was one of the largest chemical species in PM10 at this location (mean: 1.56 μg SO_4^{2-}/m^3). Factor 2 had 24.3% of the overall predicted sulphate concentration associated with it. For this reason, it was referred to as "mineral dust and sulphates". Other authors (Harrison et al., 1997; Yubero et al., 2011) also identified a mineral source from a factor in which sulphates were present. The association of SO_4^{2-} with dust minerals or metals (e.g., V) is not surprising given their similar residence time in the atmosphere (section 3.1). The sulphate concentration reached maximum levels in Factor 2 on 16 July 2014 and 26 September 2013, both characterised by a negligible rainfall on previous days. Furthermore, the three previous days were under EU in the first case and RE in the second one.

3.2.3. *Factor 3: marine aerosol*

Na, Cl^- and Mg, markers of sea-salt (Khalil and Rasmussen, 2003; Pandolfi et al., 2011), were predominant in the third factor. Thus, Factor 3 was defined as marine aerosol. This factor contributed to PM10 in 3.54 μg PM/m^3 on average (maximum: 10.48 μg PM/m^3). The importance of the apportionment of this source to PM10 at the sampling site was expected due to its location near the Bay of Biscay coastline (Fig. 1). Spanish coastal sites in the Mediterranean area registered lower annual mean values of sea spray (2.9 μg PM/m^3) than

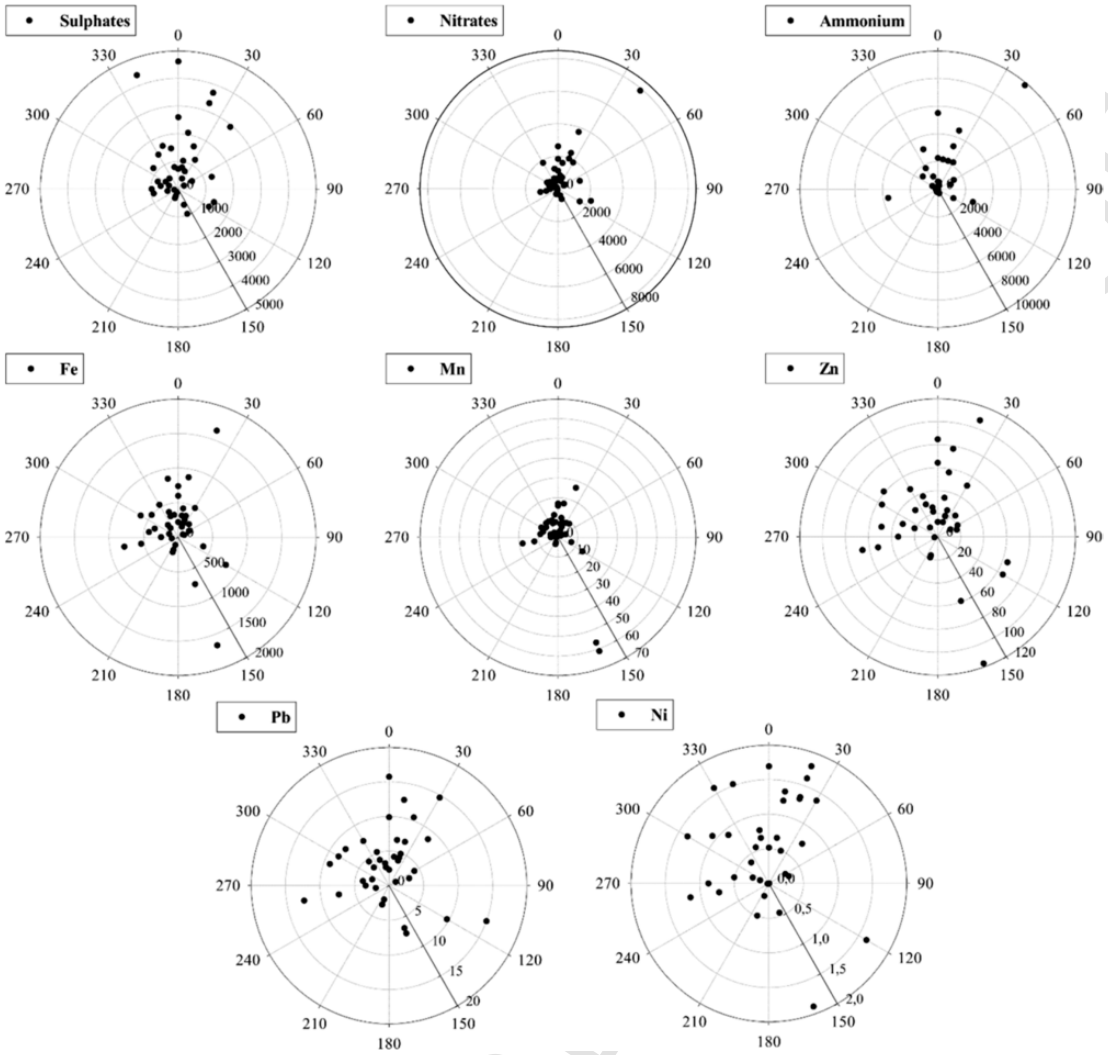

Fig. 4. Polar plots of the concentration, in ng/m^3, of SO_4^{2-}, NO_3^-, NH_4^+, Fe, Mn, Zn, Pb and Ni as a function of the direction of maximum wind speed from October 2013 to July 2014 (n = 39)[2].

those from locations on the Atlantic (Pey et al., 2009). Given the sampling location and the strong relationship between Na and Mg (R^2 = 0.86, p-value<0.01), these two elements seemed to originate from a marine source. Sr, an element present in seawater as Sr^{2+} (SEC, 2011), also presented an important loading in Factor 3, which is quite common in sea-spray factors (Alleman et al., 2005; Harrison et al., 2003). The major ions in sea-spray aerosol are Cl^-, Na^+, SO_4^{2-}, Mg^{2+}, Ca^{2+} and K^+ (SEC, 2011). Thus, K and Ca may also originate from marine sources (Srimuruganandam and Nagendra, 2012). According to the model, Factor 3 constituted the fourth main source of K and the third of Ca (11.4% and 17.5% of the total predicted K and Ca, respectively). Given marine components are mainly in the coarse fraction (Pey et al., 2009), lower contributions are expected of marine aerosol for finer fractions of PM.

No major variations were found in the concentrations of Na depending on the season. In fact, the mean in the cold period (October–March) was 1.10 μg Na/m^3 (0.17–3.72 μg Na/m^3), while in the warm period (April–September), it was 0.92 μg Na/m^3 (0.07–2.33 μg Na/m^3). The levels of Cl^- showed a more pronounced difference, however, with mean values of 1.58 μg Cl^-/m^3 in the cold period (0.37–7.16 μg Cl^-/m^3) and 0.94 μg Cl^-/m^3 in the warm period (0.06–5.18 μg Cl^-/m^3). Yi and Hwang (2014) found the marine source without the presence of chlorides, in which case it was called "aged" marine aerosol. These researches considered the lack of Cl^- as a result of a reaction between NaCl and HNO_3 and/or H_2SO_4, giving rise to Na_2SO_4, $NaNO_3$ and HCl (gas). NH_4NO_3 breaks down at high temperatures, favouring the appearance of HNO_3, which may result in greater apportionments of aged sea salt in the warmer seasons (Yubero et al., 2011). The EU guidelines for demonstrating natural sources (SEC, 2011) consider Na a better tracer of sea spray than Cl^-. According to these guidelines, sea salt is the main contributor to marine aerosol and can be calculated as 3.27 times the concentration of Na (assuming that it is only made up of NaCl), which would lead to 14.5% of PM10 being sea salt. The PCA-MLRA model explained practically all the Na (95.7% of the predicted Na, R^2 = 0.89, p-value<0.01) by means of Factor 3, forming 15.2% of the predicted PM10.

[2] Directions of maximum wind speed were only available for thirty-nine samples (section 2.4). The polar plot of Ni shows the concentration of 38 samples given that its maximum was an outlier (24.0 ng Ni/m^3 on 9 December 2013 within 110° of maximum wind speed).

Table 1
Factor loading matrix provided by PCA using varimax rotation (loadings >0.4 in bold).

Chemical species	Factor 1	Factor 2	Factor 3	Factor 4	Factor 5	Factor 6
	Road traffic	Mineral dust/Sulphates	Marine aerosol	Steelworks	Combustion	Secondary aerosol
Al_2O_3	0.100	**0.799**	0.032	0.185	0.149	0.106
Ba	**0.750**	0.393	0.029	0.207	0.117	0.102
Bi	**0.742**	0.390	0.068	0.362	0.130	0.198
Ca	**0.604**	0.387	0.331	0.303	0.244	−0.029
Ce	0.381	**0.779**	−0.064	0.096	0.070	0.162
Cl^-	0.151	−0.159	**0.844**	0.051	−0.058	−0.135
Co	0.327	0.292	−0.046	0.153	**0.824**	0.180
Cu	**0.936**	0.141	0.081	0.185	0.074	0.036
EC	**0.916**	0.030	0.103	0.202	0.119	−0.122
Fe	0.339	0.215	0.180	**0.769**	−0.013	0.006
K	**0.667**	0.309	0.263	0.117	**0.478**	0.247
La	0.215	**0.836**	0.004	0.070	0.103	0.301
Mg	−0.018	0.064	**0.960**	0.055	−0.043	0.115
Mn	0.236	0.275	−0.012	**0.713**	−0.103	−0.119
Na	−0.068	−0.076	**0.945**	0.010	−0.033	−0.046
NH_4^+	0.089	0.302	−0.137	0.048	0.092	**0.887**
Ni	0.168	0.048	−0.082	−0.001	**0.931**	0.038
NO_3^-	0.217	0.140	0.141	−0.041	0.102	**0.787**
OM	**0.759**	0.117	−0.096	0.029	**0.481**	0.121
Pb	0.218	0.167	0.066	**0.659**	0.332	0.387
Rb	0.233	**0.492**	0.150	0.385	0.398	0.203
Sb	**0.822**	0.289	0.088	0.164	0.093	0.111
Sn	**0.843**	0.066	−0.055	0.232	0.057	0.132
SO_4^{2-}	−0.123	**0.410**	−0.101	0.279	0.052	**0.689**
Sr	**0.416**	0.386	**0.724**	0.216	0.123	0.011
Ti	0.373	**0.823**	0.015	0.143	0.061	0.299
V	0.087	**0.520**	−0.142	0.331	0.094	**0.424**
Zn	0.278	0.020	0.074	**0.821**	0.138	0.176
Variance (%)	23.9	16.1	12.2	11.2	9.0	9.8
Predicted PM10 (%)	24.7	12.8	15.2	2.6	11.1	33.6

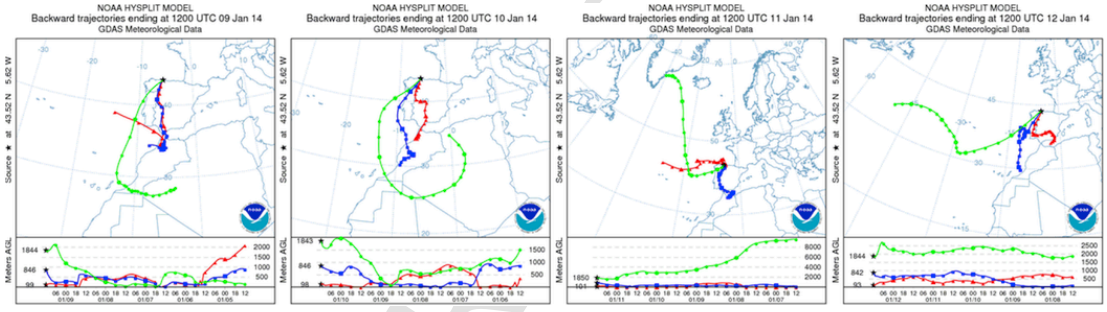

Fig. 5. Five-day air mass back trajectories during an African dust outbreak (9–12 January 2014).

3.2.4. Factor 4: steelworks

The profile of Factor 4 was mainly defined by Fe, Mn, Pb and Zn. The PCA-MLRA predicted a contribution from Factor 4 to the overall mass of each of these elements of 62%, 65%, 52% and 75%, respectively. Fernández-Olmo et al. (2016) associated Fe, Mn and Zn in PM10 with local iron foundry and casting plants. As Fe is frequently found near steelworks, this element is considered a good tracer of iron and steel manufacturing (Lin et al., 2016). Using scanning electronic microscopy with energy dispersive X-ray spectroscopy and imaging techniques, Fe-rich particles in PM10 were found in the area under study (Suárez-Peña et al., 2016). Moreover, Almeida et al. (2015) carried out a study at the steelworks located to the west of the sampling area (Fig. 1). These authors related Fe, Mn, Pb and Zn with basic oxygen steelmaking and the sinter plant. In general, the polar plots of the concentrations of these four elements as a function of the direction of maximum wind speed (Fig. 4) showed higher levels in the directions 260–30°. The steelworks were located within that sector. However, high concentrations of Fe, Mn and Zn in PM10 were recorded within 160° of the maximum wind speed (47 km/h) on 21 October 2013. That day, the five-day back trajectories of air-masses pointed to AW. Based on the above, Factor 4 was associated to steelworks.

3.2.5. Factor 5: combustion

This factor was defined by Ni, Co, K and OM. The latter chemical species played a very important role in this factor, given its high concentrations in PM10 of up to 23.07 μg OM/m^3 (mean value: 6.14 μg OM/m^3). Factor 5 maximised on 8–9 December 2013, apportioning up to 21.0 μg predicted PM10/m^3 on the second of these days (50.8% of the predicted PM10). The concentrations of the overall PM10 and K determined that day (42.6 μg PM10/m^3 and 0.45 μg K/m^3) were well above their means for the sampling period (19.1 μg PM10/m^3 and 0.17 μg K/m^3). Moreover, the maximums of OM were registered on those days: 23.1 μg OM/m^3 on 8 December 2013 and 20.7 μg OM/m^3 on 9 December 2013. K^+ is good tracer of wood and biomass combustion (Watson et al., 2001). K and Rb were found to be somewhat related (R^2 = 0.47, p-value<0.01). In fact, on 9 December 2013,

71.1% of the predicted Rb mass was explained only by Factor 5. Rb has also been associated with biomass burning (Godoy et al., 2005).

On the one hand, the facts reported above pointed to biomass combustion as a possible source to be associated with Factor 5. In fact, the period 7–11 December 2013 was identified by the Ministry of Agriculture, Food and Environment of Spain as days with a high probability of being affected by biomass combustion in forest fires (MAGRAMA, 2014). According to NAAPS, the smoke surface concentration in the northwest region of Spain varied between 1 and 16 $\mu g/m^3$ on those days (about 1–4 $\mu g/m^3$ in the area of the sampling location). Occasionally, the uncontrolled burning of stubble, bushes or natural grasses causes fires in woodlands and forest masses, which can have more or less serious environmental consequences depending on climatological conditions (humidity, wind speed, temperature …). Controlling combustion events as such is important from the point of view of preserving forests, but also to prevent major emissions of PM to the atmosphere. According to Khalil and Rasmussen (2003), combustion processes of this type involve high levels of OC, EC and K in PM and CH_3Cl, CO and H_2 in the gas phase. These authors reported much lower EC/OC ratios in the emissions originating from wood combustion than in those from vehicles or oil furnaces, given that the former occurred at a lower temperature and thus produced more OC. The EC/OC ratio obtained for Factor 1 (traffic) was 0.34, whereas for Factor 5 it was 0.06.

On the other hand, the presence of Ni and Co in Factor 5 may also indicate industrial combustion (Alharbi et al., 2015). Ni is emitted by petroleum and coal combustion and Ni–V are tracers of oil burning (Negral et al., 2008). In this study, however, these two elements did not seem to be linked, while V was associated with the secondary aerosol, as in Harrison et al. (1997). These authors found K and Ni related to coal combustion. In their case, the relationship was clearer than in the present study, as the source profile included As, which is a good tracer of this source. Padoan et al. (2016) also defined a source of fossil fuel combustion and biomass burning by K and Ni. Fig. 4 presents the polar plot of Ni as a function of the direction of maximum wind speed. The maximum concentration (24.0 ng Ni/m^3 on 9 December 2013) was not included in the polar plot as this value was an outlier compared to the rest of the dataset. In general, the highest levels came from the 300–30° sector. Considering that there was a coal-fired power station and a coalfield at a distance of less than 10 km in this sector (Fig. 1), Factor 5 could reflect the PM emissions from these facilities. Rout et al. (2015) associated a PCA factor with high loadings (>0.7) of Ni, Co and Cr with coal dust. In fact, these authors suggested that volatile elements like Co and As could be released from coal combustion, whereas non-volatiles such as Ni, Cu and Cr may originate from coal dust and ashes.

Considering all the above, Factor 5 was associated to low and high temperature combustion processes.

3.2.6. Factor 6: secondary aerosol

Given SO_4^{2-}, NO_3^- and NH_4^+ were present in Factor 6 with high loadings, this was called secondary aerosol. The presence of metals such as V and Pb in this factor has to do with their residence times in the atmosphere (section 3.2.2). Factor 6 contributed 33.6% to the overall predicted PM10 (Table 1). Although the quantification of source apportionments provided by PCA-MLRA may not be highly precise, it is clear that the contribution of secondary species to PM was quite substantial in this suburban area.

4. Conclusions

PM10 from a suburban site in the northwest of Spain was assessed using data from chemical determinations, meteorological parameters, aerosol maps, the study of five-day back trajectories of air masses and the results from a PCA-MLRA receptor model. The secondary inorganic chemical species in airborne PM were the main focus of attention.

Sulphates, nitrates and ammonium formed 16.5% of PM10 on average, in line with other suburban background sites in Europe. However, a maximum of 47.8% of PM10 was recorded after several days under the influence of air masses from Europe. These secondary species showed seasonality, with the highest concentrations of sulphates in summer and of nitrates in winter, explaining the high values of the NO_3^-/SO_4^{2-} ratio in winter (up to 2.69). Furthermore, the highest values of these two chemical species coincided with episodes of poor air circulation and influxes of air masses from Europe. The relationship between SO_4^{2-} and NH_4^+ ($R^2 = 0.57$, p-value<0.01) improved considerably in summer and spring ($R^2 = 0.88$ and $R^2 = 0.87$, respectively, p-value<0.01), while in the case of NH_4^+ and NO_3^- ($R^2 = 0.55$, p-value<0.01) in winter ($R^2 = 0.91$, p-value<0.01).

The PCA-MLRA model pointed to six relevant sources: road traffic, mineral dust and sulphates, marine aerosol, steelworks, combustion and secondary aerosol. The first source involved mixed exhaust and non-exhaust fumes and gave the same results found in a previous study carried out using a simpler technique. African dust outbreaks, characterised by an arc through the Atlantic Ocean, were usually associated with a higher Al_2O_3 concentration explained by this source. Na, Cl^- and Mg were predominant in the marine aerosol, with Cl^- showing differences between the cold and the warm period of the year. The results of the model were compared with another study carried out at nearby steelworks to associate Fe, Mn, Pb and Zn with its activities (basic oxygen steelmaking and sinter plant). Finally, major amounts of PM were released to the atmosphere coinciding with episodes of biomass burning in forest fires. On isolated days, combustion was found to contribute large emissions of PM to the atmosphere, up to 21 $\mu g\ PM/m^3$ (50.8% of PM10). The contribution from industrial processes to this source cannot be ruled out given the presence of Ni and Co in its profile.

Results evidenced the relevance of stationary and mobile sources in the air quality at the suburban site under study, with important apportionments of PM originating from road traffic and as consequence of the release of precursor gases of secondary participles to the atmosphere.

Acknowledgements

The authors gratefully acknowledge funding from the Principality of Asturias Regional Government (project SV-PA-13-ECOEMP-65). An acknowledgment is given to the Spanish Meteorological Agency (AEMET) for the information provided, the University of Athens for the SKIRON model (http://forecast.uoa.gr/dustindx.php), the Barcelona Supercomputing Center (http://www.bsc.es/projects/earthscience/BSC-DREAM/) for the BSC-DREAMS8b (Dust Regional Atmospheric Model) model, the Naval Research Laboratory Monterey for the NAAPS (Navy Aerosol Analysis and Prediction System) Global Aerosol Model administrated by the Naval Research Laboratory (NRL), and the NOAA Air Resources Laboratory (ARL) for the HYSPLIT model (http://www.ready.noaa.gov).

Appendix A. Supplementary data

Supplementary data related to this article can be found at http://dx.doi.org/10.1016/j.jenvman.2016.12.032.

Uncited reference

PRTR-Spain, 2016.

References

Alharbi, B., Shareef, M.M., Husain, T., 2015. Study of chemical characteristics of particulate matter concentrations in Riyadh. Saudi Arabia. Atmos. Pollut. Res. 6, 88–98. http://dx.doi.org/10.5094/APR.2015.011.

Alleman, L.Y., Lamaison, L., Perdrix, E., Robache, A., Galloo, J.C., 2010. PM10 metal concentrations and source identification using positive matrix factorization and wind sectoring in a French industrial zone. Atmos. Res. 96, 612–625. http://dx.doi.org/10.1016/j.atmosres.2010.02.008.

Almeida, S.M., Lage, J., Fernández, B., Garcia, S., Reis, M.A., Chaves, P.C., 2015. Chemical characterization of atmospheric particles and source apportionment in the vicinity of a steelmaking industry. Sci. Total Environ. 521, 411–420. http://dx.doi.org/10.1016/j.scitotenv.2015.03.112.

Amato, F., Alastuey, A., Karanasiou, A., Lucarelli, F., Nava, S., Calzolai, G., Severi, M., Becagli, S., Gianelle, V., Colombi, C., Alves, C., Custódio, D., Nunes, T., Cerqueira, M., Pio, C., Eleftheriadis, K., Diapouli, E., Reche, C., Minguillón, M.C., Manousakas, M.I., Maggos, T., Vratolis, S., Harrison, R.M., Querol, X., 2016. AIRUSE-LIFE+: a harmonized PM speciation and source apportionment in five southern European cities. Atmos. Chem. Phys. 16, 3289–3309. http://dx.doi.org/10.5194/acp-16-3289-2016.

Belis, C.A., Karagulian, F., Larsen, B.R., Hopke, P.K., 2013. Critical review and meta-analysis of ambient particulate matter source apportionment using receptor models in Europe. Atmos. Environ. 69, 94–108. http://dx.doi.org/10.1016/j.atmosenv.2012.11.009.

Di Gilio, A., De Gennaro, G., Dambruoso, P., Ventrella, G., 2015. An integrated approach using high time-resolved tools to study the origin of aerosols. Sci. Total Environ. 530, 28–37. http://dx.doi.org/10.1016/j.scitotenv.2015.04.073.

Fernández-Camacho, R., de la Rosa, J.D., Sánchez de la Campa, A.M., 2016. Trends and sources vs air mass origins in a major city in South-western Europe: implications for air quality management. Sci. Total Environ. 553, 305–315. http://dx.doi.org/10.1016/j.scitotenv.2016.02.079.

Fernández-Olmo, I., Andecochea, C., Ruiz, S., Fernández-Ferreras, J.A., Irabiena, A., 2016. Local source identification of trace metals in urban/industrial mixed land-use areas with daily PM10 limit value exceedances. Atmos. Res. 171, 92–106. http://dx.doi.org/10.1016/j.atmosres.2015.12.010.

Gobierno del Principado de Asturias, 2014. Plan de mejora de la calidad del aire en la aglomeración de Gijón ES0304. Consejería de Fomento, Ordenación del Territorio y Medio Ambiente. Online at: https://www.asturias.es/medioambiente/articulos/ficheros/PLAN_MEJORA_CALIDAD_DEL_AIRE_GIJON.pdf (Accessed 5 June 2016).

Godoy, M.L.D.P., Godoy, J.M., Artaxo, P., 2005. Aerosol source apportionment around a large coal fired power plant – thermoelectric Complex Jorge Lacerda, Santa Catarina, Brazil. Atmos. Environ. 39, 5307–5324. http://dx.doi.org/10.1016/j.atmosenv.2005.05.033.

Harrison, R.M., Smith, D.J.T., Pio, C.A., Castro, L.M., 1997. Comparative receptor modelling study of airborne particulate pollutants in Birmingham (United Kingdom), Coimbra (Portugal) and Lahore (Pakistan). Atmos. Environ. 31, 3309–3321. http://dx.doi.org/10.1016/S1352-2310(97)00152-0.

Harrison, R.M., Tilling, R., Callén Romero, M.S., Harrad, S., Jarvis, K., 2003. A study of trace metals and polycyclic aromatic hydrocarbons in the roadside environment. Atmos. Environ. 37, 2391–2402. http://dx.doi.org/10.1016/S1352-2310(03)00122-5.

Jorquera, H., Barraza, F., 2013. Source apportionment of PM_{10} and $PM_{2.5}$ in a desert region in northern Chile. Sci. Total Environ. 444, 327–335. http://dx.doi.org/10.1016/j.scitotenv.2012.12.007.

Khalil, M.A.K., Rasmussen, R.A., 2003. Tracers of wood smoke. Atmos. Environ. 37, 1211–1222. http://dx.doi.org/10.1016/S1352-2310(02)01014-2.

Li, H., Duan, F., He, K., Ma, Y., Kimoto, T., Huang, T., 2016. Size-dependent characterization of atmospheric particles during winter in Beijing. Atmosphere 7 (36)http://dx.doi.org/10.3390/atmos7030036.

Lin, Y.C., Hsu, S.C., Chou, C.C.K., Zhan, R., Wu, Y., Kao, S.J., Luo, L., Huang, C.H., Lin, S.H., Huang, Y.T., 2016. Wintertime haze deterioration in Beijing by industrial pollution deduced from trace metal fingerprints and enhanced health risk by heavy metals. Environ. Pollut. 208, 284–293. http://dx.doi.org/10.1016/j.envpol.2015.07.044.

MAGRAMA, 2014. Episodios naturales de partículas 2013. CSIC, AEMET, CIEMAT, Ministerio de Agricultura, Alimentación y Medio Ambiente, Subdirección General de Calidad del Aire y del Medio Ambiente Industrial. Online at: http://www.magrama.gob.es/es/calidad-y-evaluacion-ambiental/temas/atmosfera-y-calidad-del-aire/Episodios_Naturales_2013_tcm7-323494.pdf (Accessed 27 May 2016).

MAGRAMA, 2015. Episodios naturales de partículas 2014. CSIC, AEMET, CIEMAT, Ministerio de Agricultura, Alimentación y Medio Ambiente, Subdirección General de Calidad del Aire y del Medio Ambiente Industrial. Online at: http://www.magrama.gob.es/es/calidad-y-evaluacion-ambiental/temas/atmosfera-y-calidad-del-aire/episodiosnaturales2014_tcm7-379247.pdf (Accessed 27 May 2016).

Megido, L., Negral, L., Castrillón, L., Marañón, E., Fernández-Nava, Y., Suárez-Peña, B., 2016a. Traffic tracers in a suburban location in northern Spain: relationship between carbonaceous fraction and metals. Environ. Sci. Pollut. R. 23, 8669–8678. http://dx.doi.org/10.1007/s11356-015-5955-8.

Megido, L., Negral, L., Castrillón, L., Suárez-Peña, B., Fernández-Nava, Y., Marañón, E., 2016b. Geochemical ratios to assess the anthropogenic influence in PM10. Environ. Sci. Pollut. R. http://dx.doi.org/10.1007/s11356-016-7858-8.

Megido, L., Suárez-Peña, B., Negral, L., Castrillón, L., Suárez, S., Marañón, E., Fernández-Nava, Y., 2016c. Relationship between physico-chemical characteristics and potential toxicity of PM10. Chemosphere 162, 73–79. http://dx.doi.org/10.1016/j.chemosphere.2016.07.067.

Negral, L., Moreno-Grau, S., Moreno, J., Querol, X., Viana, M.M., Alastuey, A., 2008. Natural and anthropogenic contributions to PM10 and PM2.5 in an urban area in the Western Mediterranean Coast. Water Air Soil Poll. 192, 227–238. http://dx.doi.org/10.1007/s11270-008-9650-y.

Negral, L., Moreno-Grau, S., Querol, X., Moreno, J., Viana, M., García-Sánchez, A., Alastuey, A., Moreno-Clavel, J., 2012. Weak pressure gradient over the Iberian Peninsula and African dust outbreaks. A new dust long-transport scenario. B. Am. Meteorol. Soc. 93, 1125–1132. http://dx.doi.org/10.1175/BAMS-D-10-05000.1.

Padoan, E., Malandrino, M., Giacomino, A., Grosa, M.M., Lollobrigida, F., Martini, S., Abollino, O., 2016. Spatial distribution and potential sources of trace elements in PM_{10} monitored in urban and rural sites of Piedmont Region. Chemosphere 145, 495–507. http://dx.doi.org/10.1016/j.chemosphere.2015.11.094.

Pandolfi, M., Gonzalez-Castanedo, Y., Alastuey, A., de la Rosa, J.D., Mantilla, E., Sanchez de la Campa, A., Querol, X., Pey, J., Amato, F., Moreno, T., 2011. Source apportionment of PM_{10} and $PM_{2.5}$ at multiple sites in the strait of Gibraltar by PMF: impact of shipping emissions. Environ. Sci. Pollut. R. 18, 260–269. http://dx.doi.org/10.1007/s11356-010-0373-4.

Pérez, N., Pey, J., Reche, C., Cortés, J., Alastuey, A., Querol, X., 2016. Impact of harbour emissions on ambient PM_{10} and $PM_{2.5}$ in Barcelona (Spain): evidences of secondary aerosol formation within the urban area. Sci. Total Environ. 571, 237–250. http://dx.doi.org/10.1016/j.scitotenv.2016.07.025.

Pey, J., Querol, X., Alastuey, A., 2009. Variations of levels and composition of PM_{10} and $PM_{2.5}$ at an insular site in the Western Mediterranean. Atmos. Res. 94, 285–299. http://dx.doi.org/10.1016/j.atmosres.2009.06.006.

PRTR-Spain, Spanish Register of Emissions and Pollutant Sources. Online at: http://www.en.prtr-es.es/Informes/InventarioInstalacionesIPPC.aspx (Accessed 5 June 2016).

Qadir, R.M., Schnelle-Kreis, J., Abbaszade, G., Arteaga-Salas, J.M., Diemer, J., Zimmermann, R., 2014. Spatial and temporal variability of source contributions to ambient PM_{10} during winter in Augsburg, Germany using organic and inorganic tracers. Chemosphere 103, 263–273. http://dx.doi.org/10.1016/j.chemosphere.2013.12.015.

Rout, T.K., Masto, R.E., Padhy, P.K., Ram, L.C., George, J., Joshi, G., 2015. Heavy metals in dusts from commercial and residential areas of Jharia coal mining town. Environ. Sci. Pollut. R. 73, 347–359. http://dx.doi.org/10.1007/s12665-014-3429-9.

SEC, 2011. Commission Staff Working Paper. Establishing Guidelines for Demonstration and Subtraction of Exceedances Attributable to Natural Sources under the Directive 2008/50/EC on Ambient Air Quality and Cleaner Air for Europe. Online at: http://ec.europa.eu/environment/air/quality/legislation/pdf/sec_2011_0208.pdf (Accessed 27 May 2016).

Schaubroeck, T., Deckmyn, G., Giot, O., Campioli, M., Vanpoucke, C., Verheyen, K., Rugani, B., Achten, W., Verbeeck, H., Dewulf, J., Muys, B., 2016. Environmental impact assessment and monetary ecosystem service valuation of an ecosystem under different future environmental change and management scenarios; a case study of a Scots pine forest. J. Environ. Manag. 173, 79–94. http://dx.doi.org/10.1016/j.jenvman.2016.03.005.

Srimuruganandam, B., Nagendra, S.M.S., 2012. Source characterization of PM_{10} and $PM_{2.5}$ mass using a chemical mass balance model at urban roadside. Sci. Total Environ. 433, 8–19. http://dx.doi.org/10.1016/j.scitotenv.2012.05.082.

Stein, A.F., Draxler, R.R., Rolph, G.D., Stunder, B.J.B., Cohen, M.D., Ngan, F., 2015. NOAA's HYSPLIT atmospheric transport and dispersion modeling system. B. Am. Meteorol. Soc. 96, 2059–2077. http://dx.doi.org/10.1175/BAMS-D-14-00110.1.

Suárez-Peña, B., Negral, L., Castrillón, L., Megido, L., Marañón, E., Fernández-Nava, Y., 2016. Imaging techniques and scanning electron microscopy as tools for characterizing a Si-based material used in air monitoring applications. Materials 9, http://dx.doi.org/10.3390/ma9020109.

Sun, Y.L., Wang, Z.F., Du, W., Zhang, Q., Wang, Q.Q., Fu, P.Q., Pan, X.L., Li, J., Jayne, J., Worsnop, D.R., 2015. Long-term real-time measurements of aerosol par

ticle composition in Beijing, China: seasonal variations, meteorological effects, and source analysis. Atmos. Chem. Phys. 15, 10149–10165. http://dx.doi.org/10.5194/acp-15-10149-2015.

Taiwo, A.M., Harrison, R.M., Shi, Z., 2014. A review of receptor modelling of industrially emitted particulate matter. Atmos. Environ 97, 109–120. http://dx.doi.org/10.1016/j.atmosenv.2014.07.051.

Watson, J.G., Chow, J.C., Houck, J.E., 2001. $PM_{2.5}$ chemical source profiles for vehicle exhaust, vegetative burning, geological material, and coal burning in Northwestern Colorado during 1995. Chemosphere 43, 1141–1151. http://dx.doi.org/10.1016/S0045-6535(00)00171-5.

Yi, S.M., Hwang, I., 2014. Source identification and estimation of source apportionment for ambient PM_{10} in Seoul, Korea. Asian J. Atmos. Environ. 8, 115–125. http://dx.doi.org/10.5572/ajae.2014.8.3.115.

Yubero, E., Carratalá, A., Crespo, J., Nicolás, J., Santacatalina, M., Nava, S., Lucarelli, F., Chiari, M., 2011. PM_{10} source apportionment in the surroundings of the San Vicente del Raspeig cement plant complex in southeastern Spain. Environ. Sci. Pollut. R. 18, 64–74. http://dx.doi.org/10.1007/s11356-010-0352-9.